Electronic Supplementary Material (ESI) for Journal of Materials Chemistry A.

Electronic Supplementary Information (ESI)

Molten-Salt Electrochemical Biorefinery for Carbon-Neutral Utilization of Biomass

Jing Wang,[a] Juanxiu Xiao,[b]* Yijun Shen,[b] Xinxin Liang,[a] Teng Lv,[a] Wei Xiao*[a]

a. *College of Chemistry and Molecular Sciences, Hubei Key Laboratory of Electrochemical Power Sources, Wuhan University, Wuhan 430072, P. R. China.*
b. *State Key Laboratory of Marine Resource Utilization in South China Sea, Hainan University, No. 58, Renmin Avenue, Haikou, Hainan, 570228, P.R. China*

*Corresponding authors.
E-mail address: 00030042@whu.edu.cn (W. Xiao); xiaojuanxiu@hainanu.edu.cn (J. Xiao)

Experimental Procedures

Materials: Rice husks (RHs) were supplied by a farm in Wuhan City, which were purified by deionized water, then dried at 80°C for 24 h, and finally crushed into powders (60 mesh) by a FZ 102 plant crusher. $CaCl_2$ (anhydrous, 99% purity), NaCl (anhydrous, 99% purity), NaClO (12% purity), CH_3COOH (99.7% purity), H_2SO_4 (98% purity) and AgCl (99.5% purity), N, N-dimethylformamide (C_3H_7NO, DMF, 99.7% purity) were obtained from Sinopharm Chemical Reagent Co., Ltd. Porous nickel (99.9% purity), molybdenum net (99.95% purity) and Graphite rod (99.995% purity) were provided by Dongguan Zehui New Material Technology co. LTD. KCl-saturated Ag/AgCl electrode was provided by Tianjin Aida Hengsheng Technology Development Co. Ltd. Fluorine-doped tin oxide (FTO)-coated glass substrates were purchased from Wuhan Jinge-Solar Energy Technology Co, Ltd. All the reagents were of analytical grade and were used without further purification. Deionized water used in the whole processes.

Acid treatment of RHs: Acid treatment of RHs: The acid solution for treating RHs was prepared by mixing 150 ml NaClO (1.61 mol/L), 100 ml CH_3COOH (16.65 mol/L) and 150 ml deionized water. Then, 400 mL of the as-prepared acid solution containing 20 g RHs powders were sealed in a blue-cap bottle and kept at 100 °C for 1 h. After cooled to room temperature, the solid residue was obtained after centrifugation for several times. The leaching process in the NaClO-CH_3COOH mixed acid solution was repeated for five times. Then, the residue was transferred into the dilute sulfuric solution (prepared by mixing 140 mL deionized water and 260 mL H_2SO_4) and kept at 50 °C for 40 min. Finally, the insoluble residue was obtained by centrifugation, followed by washing in deionized water and absolute ethanol and dried at 60 °C for 12 h. The resulting product is denoted as A-RHs.

Calculation on energy consumption: The energy consumption (E_c, kWh kg^{-1}) was calculated by the following equation:

$$E_c = \frac{U \times \int I dt}{m}$$

where m (g) is the mass of obtained SiC and Si, respectively. I (A) is the electrolysis current. t (s) is the electrolysis time and U (2.6 V) is the electrolysis voltage.

Calculation of work function: The work function of probe is calibrated to be 4.25 eV by the highly oriented pyrolytic graphite as a standard reference surface. The work function (W) of the samples were calculated via the equation below:

$$W_{sample} = W_{probe} + e \times CPD_{sample}$$

where W_{sample} and W_{probe} are the work functions of the corresponding sample and gold tip (= 4.25 eV), e is the electronic charge, and CPD_{sample} is the obtained CPD value of the samples.

Then, the Fermi levels (E_f) of the samples are estimated as follows:

$$E_f = E_{vac} - W_{sample}$$

where E_{vac} is the energy of static electron at the vacuum level (assumed as 0 eV).

The apparent quantum yields (AQYs) for the catalysts were tested under the same reaction conditions except the wavelengths of the incident light, and calculated by the following equation.

$$AQY = \frac{2 \times \text{the number of CO molecules} + 8 \times \text{the number of } CH_4 \text{ molecules}}{\text{the number of incident photos}} \times 100\%$$

$^{13}CO_2$ isotope experiments: Controlled isotope-labeled photocatalytic tests were conducted by replacing $^{12}CO_2$ with $^{13}CO_2$ while keeping other reaction conditions unchanged. The obtained products were analyzed by gas chromatography–mass spectrometry (GCMS-QP2020NX, SHIMADZU) equipped with SH-Rt-Msieve 5A columna. He was used as the carrier gas (0.5 mL min^{-1}), the forward inlet temperature was 190 °C, the chromatographic column temperature was 45 °C, and the detector temperature was 200°C.

Charge flow tracking by photo-deposition: Photo-deposition of 1.5wt % Pt on the surfaces of SiC/C/Ag-5 carried out using H_2PtCl_6 as precursors, respectively. Typically, 20 mg of SiC/C/Ag-5 and a calculated amount of the metal precursor were mixed in 50 mL ethanol (10 vol%) aqueous solution with stirring. The suspension was then irradiated by a 300 W Xe lamp with the reaction temperature maintained at 0°C by cycle cooling water equipment. After 1 h of photo-deposition, the suspension was filtered, washed several times with deionized water, and finally dried in the vacuum oven at 60°C overnight.

Life cycle assessment methods

Functional unit: The functional unit is defined as the production of 1 metric ton of SiC/C and SiC/C/Ag-5.

System boundary: The research path includes four stages: rice production, raw material extraction and photocatalysts production. The impact of plant construction and equipment maintenance was excluded and it is assumed that the electrolyte is not consumed during the electrolysis process. Some processes, such as transportation and heat loss, were excluded from the study. All electricity consumed in the life cycle assessment process is based on thermal power generation.

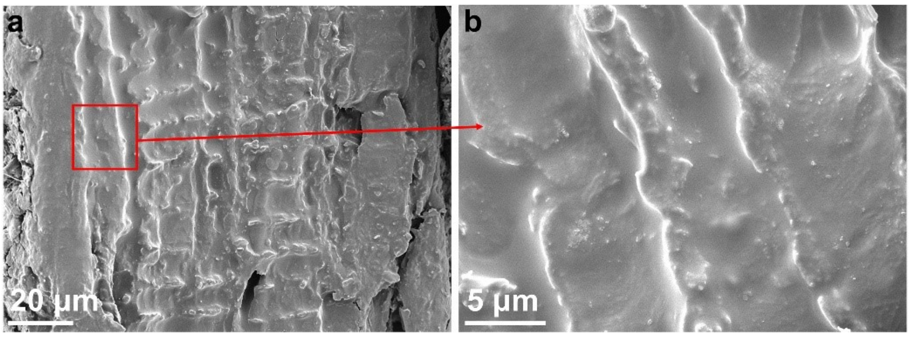

Fig. S1. The SEM images of the rice husks.

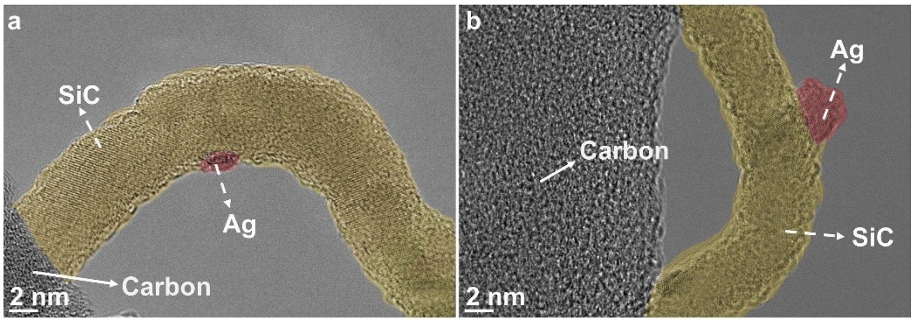

Fig. S2. HRTEM images of the SiC/C/Ag-5.

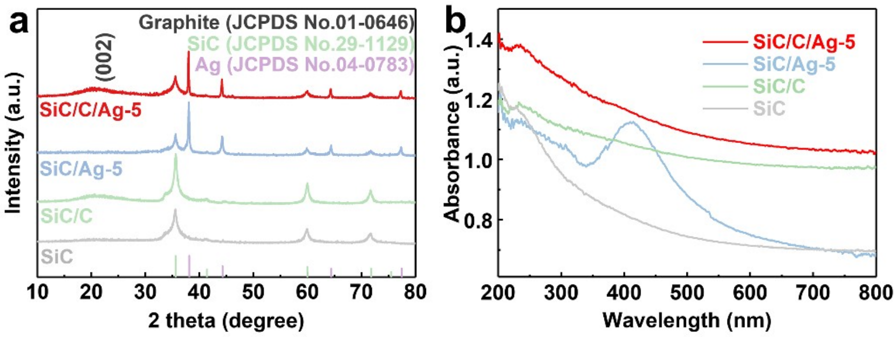

Fig. S3. (a) XRD patterns and (b) UV–vis DRS of SiC, SiC/C, SiC/Ag-5 and SiC/C/Ag-5.

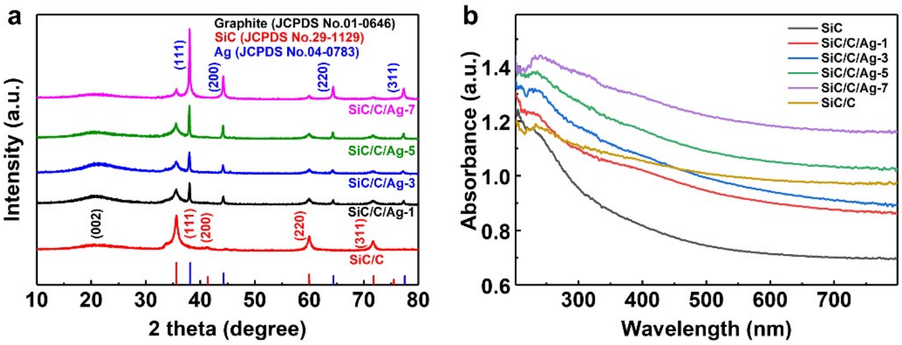

Fig. S4. (a) XRD patterns and (b) UV–vis DRS of samples.

Table S1. Contents of Ag for SiC/C/Ag-1, SiC/C/Ag-3, SiC/C/Ag-5 and SiC/C/Ag-7.

Sample	Ag (wt.%)
SiC/C/Ag-1	0.15
SiC/C/Ag-3	0.39
SiC/C/Ag-5	0.67
SiC/C/Ag-7	0.93

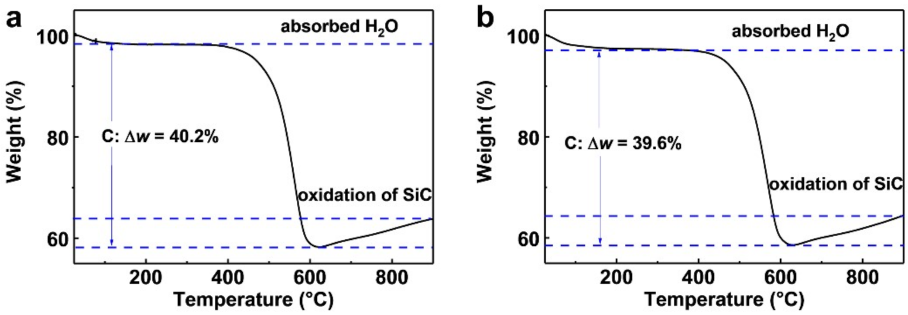

Fig. S5. TGA curve of (a) SiC/C/Ag -5 and (b) SiC/C in air.

The carbon content of SiC/C/Ag-5 and SiC/C was determined by the TGA. As shown in Fig. S5, the weight loss before 200 °C is ascribed to the moisture. In the range of 300~620 °C, carbon react with oxygen in air to produce carbon dioxide. The content of carbon in SiC/C/Ag-5 and SiC/C is 40.2 wt.% and 39.6 wt.%, respectively. The content of Ag in SiC/C/Ag-5 is 0.67 wt.%, was measured by ICP-OES (Table S1). Therefore, the SiC content in SiC/C/Ag-5 and SiC/C is calculated to be around 59.13 wt.% and 60.40 wt.%, respectively (Table S2).

Table S2. Contents of SiC, C and Ag for SiC/C/Ag-5 and SiC/C.

Sample	SiC (wt.%)	C (wt.%)	Ag (wt.%)
SiC/C/Ag-5	59.13	40.20	0.67
SiC/C	60.40	39.60	0

Table S3. Contents of typical impurities in the RHs and SiC/C/Ag-5 determined by ICP-OES.

Sample	K (ppm)	Mg (ppm)	S (ppm)	P (ppm)
RHs	2385	493	416	495
SiC/C/Ag-5	89	196	53	347
Removal ratio	99%	94%	98%	88%

$$\text{Removal ratio} = \left(1 - \frac{\text{Total mass in 163 mg SiC/C/Ag - 5}}{\text{Total mass in 1000 mg RHs}}\right) \times 100\%$$

Note: The mass of K, Mg, S and P in 1000 mg of RHs is 2.385, 0.493, 0.416 and 0.495 mg, respectively. 1000 mg of RHs can finally produce 163 mg of SiC/C/Ag-5 by the molten salt electrolysis. Correspondingly, the total mass of K, Mg, S and P in the obtained 163 mg of SiC-NW/C is 0.015, 0.032, 0.009 and 0.057 mg, respectively. Therefore, after the molten salt treatment, the removal ratios of K, Mg, S and P are 99, 94, 98 and 88 % (Table S3), respectively.

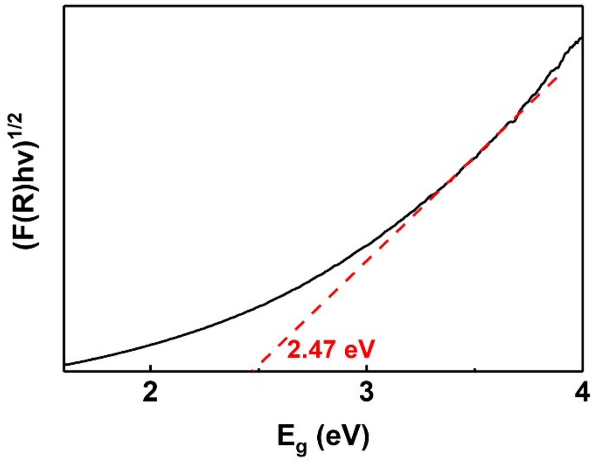

Fig. S6. Tauc plot of SiC.

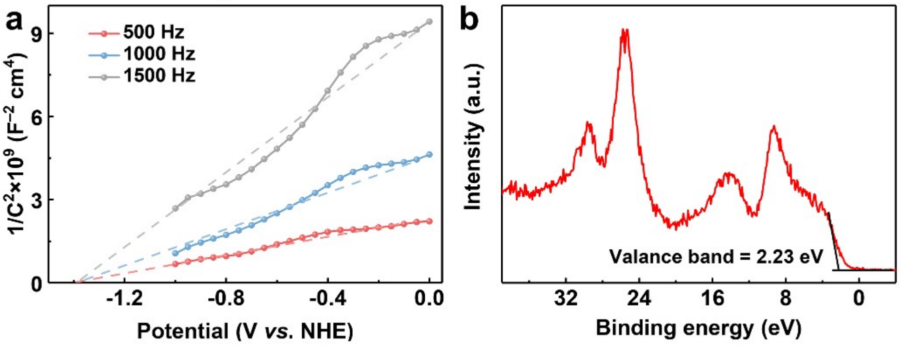

Fig. S7. (a) Mott-Schottky plot of SiC and (b) VB XPS of SiC.

VB_{SiC} = the flat-band potential + the XPS-VB potential = -1.39 V + 0.059 pH + 2.23 V = 1.25 V vs. NHE, pH = 7.

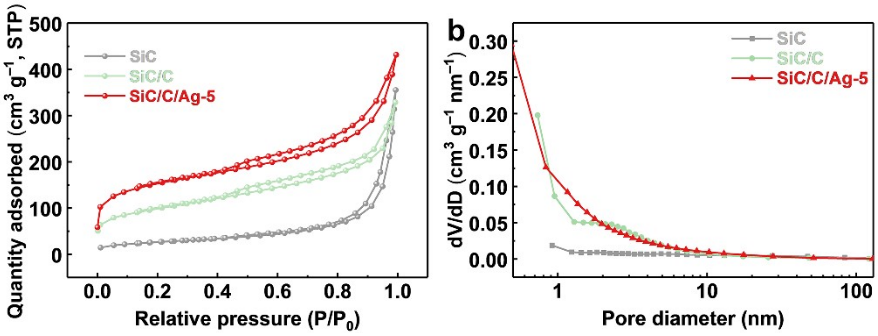

Fig. S8. (a) N_2 sorption isotherms and (b) Pore size distribution curves of SiC, SiC/C and SiC/C/Ag-5 at 77 K.

Table S4. Comparison of specific surface area and total pore volume of SiC, SiC/C and SiC/C/Ag-5.

Sample	Specific surface area (m^2 g^{-1})	Total pore volume (cm^3 g^{-1})
SiC	96	0.55
SiC/C	352	0.64
SiC/C/Ag-5	545	0.68

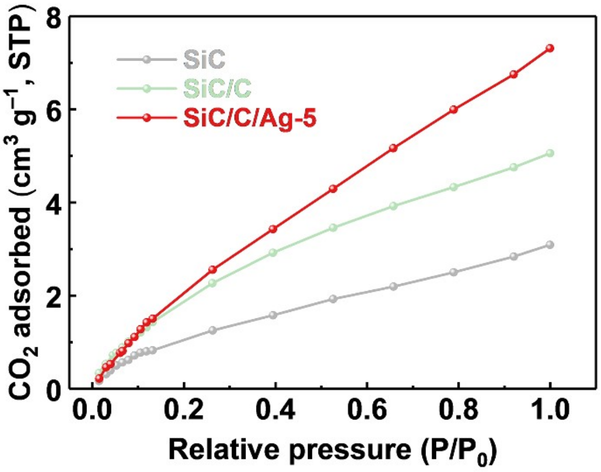

Fig. S9. CO$_2$ adsorption isotherms of SiC, SiC/C and SiC/C/Ag-5 at 273 K.

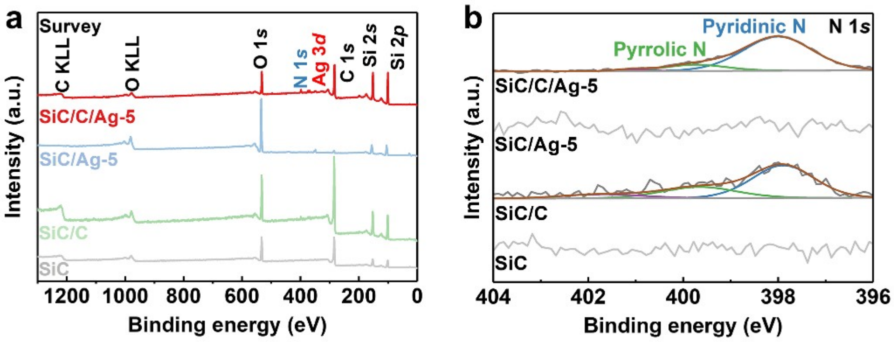

Fig. S10. (a) XPS survey spectra, (b) high resolution N 1*s* XPS spectra of SiC, SiC/C, SiC/Ag-5 and SiC/C/Ag-5.

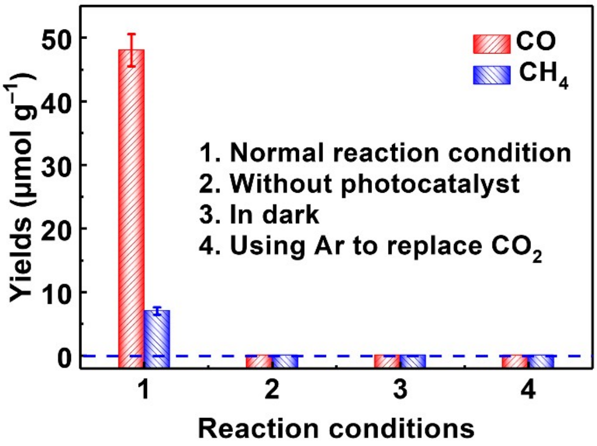

Fig. S11. Activity of reaction system under various conditions for 3 h.

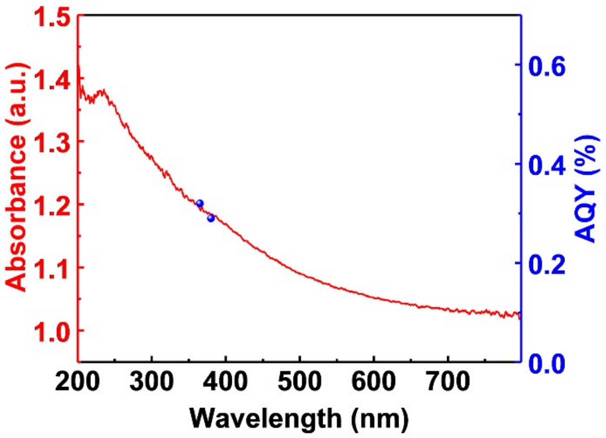

Fig. S12. DRS spectrum of SiC/C/Ag-5 composite (left axis) and AQY versus the incident light wavelength (right axis).

Table S5. Comparison of photocatalytic reduction performance of gaseous CO_2.

Photocatalyst	Light source	Main product ($\mu mol\ g^{-1}\ h^{-1}$)	Ref.
SiC/C/Ag	300 W Xe lamp (320-780 nm)	CO 16.0 CH_4 2.33	This work
SiC/C	300 W Xe lamp (320-780 nm)	CO 5.87 CH_4 0.37	[1]
$Ta_3N_5/LaTiO_2N$	300 W Xe lamp ($\lambda > 420$ nm)	CO 11.53 CH_4 2.32	[2]
TiO_2	300 W Xe lamp (320-780 nm)	CH_4 1.35	[3]
TaON@G	300 W Xe lamp ($\lambda > 420$ nm)	CH_4 1.61	[4]
$La_2O_3/LaTiO_2N$	300 W Xe lamp ($\lambda > 420$ nm)	CH_4 0.98	[5]
$Pt/CeO_2/MnO_x$	300 W Xe lamp (320-780 nm)	CH_4 1.12	[6]
ZnAl-LDH	300 W Xe lamp (320-780 nm)	CO 7.6	[7]
$Cu_3(BTC)_2$@TiO_2	300 W Xe lamp ($\lambda < 400$ nm)	CH_4 2.64	[8]
Mg-In LDH	200 W Hg-Xe lamp (UV-vis)	CO 3.21	[9]
$BiOBr_xCl_{1-x}$	300 W Xe lamp simulate sun light	CO 15.86	[10]

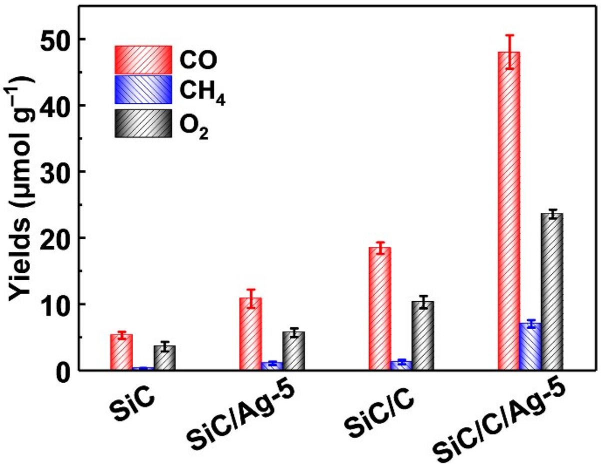

Fig. S13. The photocatalytic activity of samples for CO_2 reduction under illumination for 3 h.

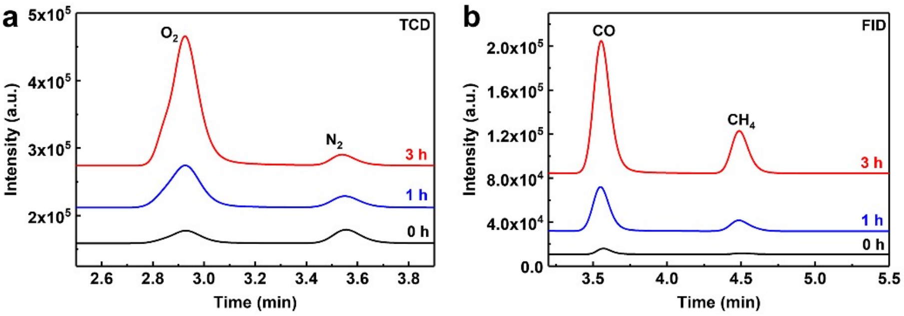

Fig. S14. Gas chromatograph spectra during photocatalytic CO_2 reduction reaction catalyzed by SiC/C/Ag-5: (a) O_2 and N_2 detected by thermal conductivity detector (TCD), (b) CO and CH_4 detected by flame ionization detector (FID).

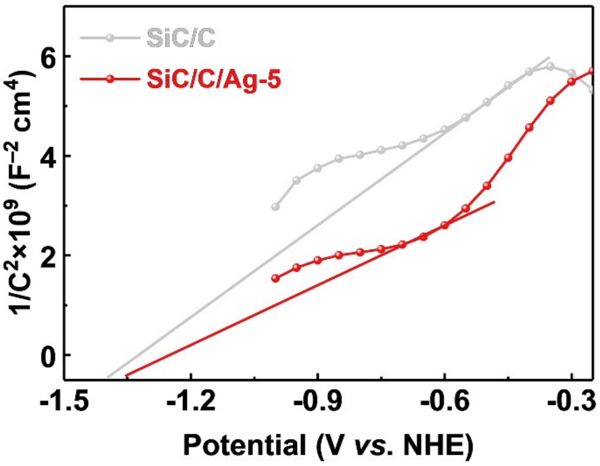

Fig. S15. Mott-Schottky plots of SiC/C and SiC/C/Ag-5 at frequencies of 1.0 kHz under simulated solar light irradiation.

Mott-Schottky analysis was used to provide fundamental insights into the charge carriers density (N_D) according to the following equation: [11]

$$N_D = \frac{2}{e\varepsilon\varepsilon_0}\left(\frac{d\left(1/C^2\right)}{dV}\right)^{-1}$$

where e is the elementary electronic charge, ε is the dielectric constant (9.72 for SiC [12]), ε_0 is the permittivity in vacuum, C is the capacitance, and V is the applied potential.

Table S6. Charge carrier density (N_D) analysis for SiC/C and SiC/C/Ag-5.

Sample	N_D (10^{21} cm^{-3})
SiC/C	4.21
SiC/C/Ag-5	6.29

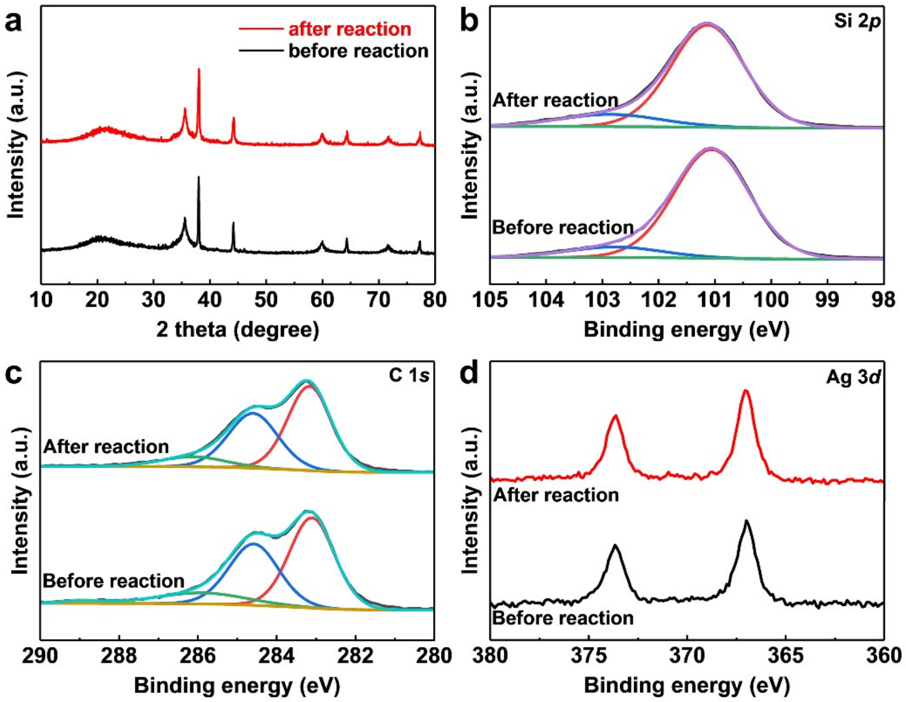

Fig. S16. (a) XRD patterns, (b) Si 2*p*, (c) C 1*s* and (d) Ag 3*d* XPS spectra of SiC/C/Ag-5 before and after five photocatalytic CO_2 reduction cycles.

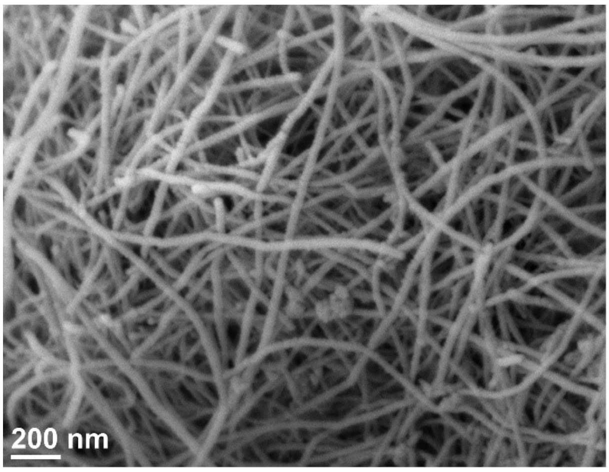

Fig. S17. The SEM images of SiC/C/Ag-5 after five photocatalytic CO_2 reduction cycles.

Table S7. The data of time-resolved fluorescence.

Sample	τ_1 (ns)		τ_2 (ns)		τ_3 (ns)		Ave.
	Value/ns	Rel%	Value/ns	Rel%	Value/ns	Rel%	τ(ns)
SiC	0.18	49.39	0.18	50.17	0.09	0.44	0.18
SiC/C	0.09	24.59	0.31	49.84	0.94	25.57	0.21
SiC/C/Ag-5	0.93	32.34	31.09	3.63	0.38	64.02	0.49

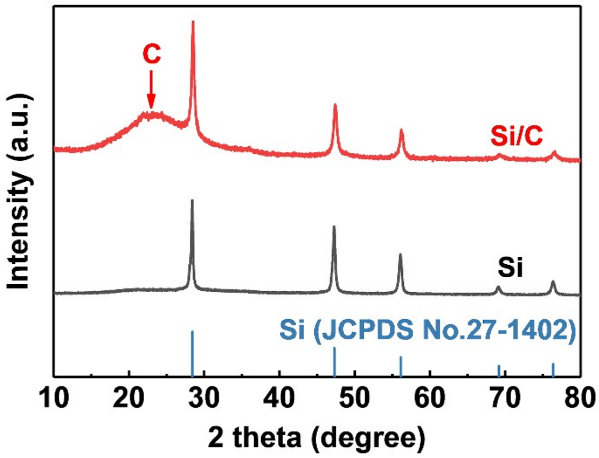

Fig. S18. XRD patterns Si/C and Si

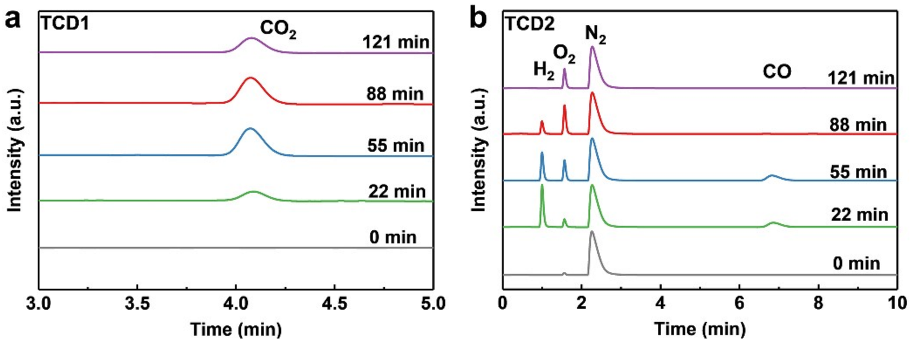

Fig. S19. Gas chromatograph spectra during electrolysis of RHs: (a) CO_2 detected by TCD1, (b) H_2, O_2, N_2 and CO detected by TCD2.

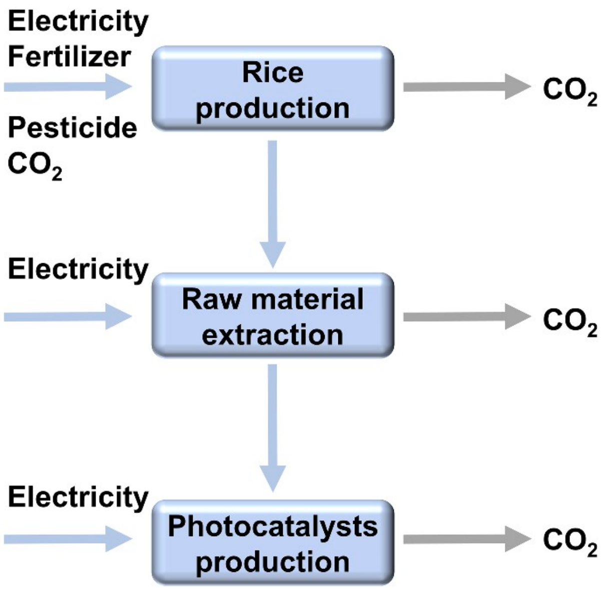

Fig. S20. Boundary division of photocatalysts production.

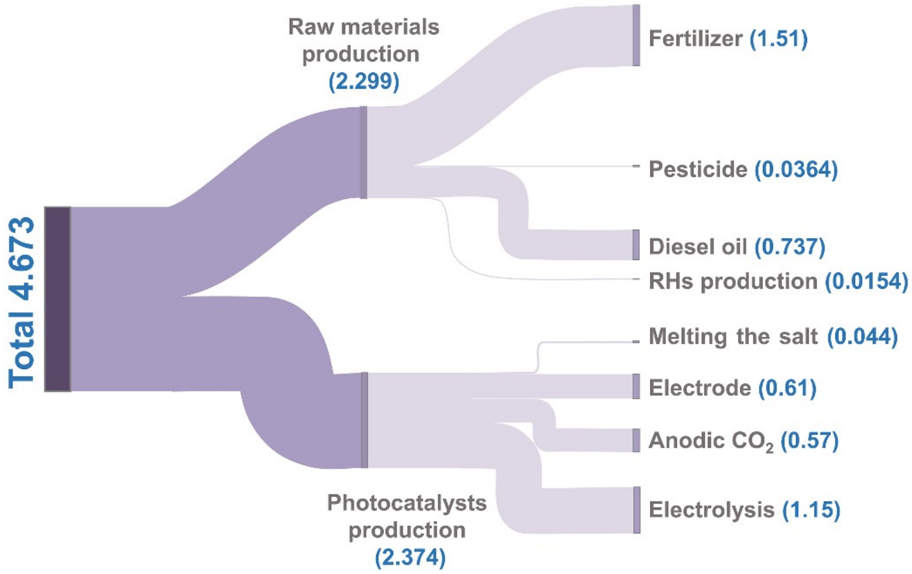

Fig. S21. Equivalent CO_2 emissions of photocatalysts production. The calculation details are provided in Fig. S20 and Table S9.

Table S8. Calculations details of LCA for the SiC/C/Ag-5 photocatalyst production.

Content	CO_2 equivalent emission (t_{CO_2} $t_{SiC/C/Ag\text{-}5}^{-1}$)	Note
CO_2 fixed by rice husk production	−4.51	The carbon content in RHs is 20.5 wt.%, production of 1 kg RHs needs 0.7517 kg CO_2. [1]
Fertilizer	1.51	Production of 1 t RHs needs 4 t rice theoretically, production of 1 t photocatalysts needs 6 t RHs.[13] Production of 1 t RHs needs 59.07 kg fertilizer, equaling to 251.42 kg CO_2 emissions. [14]
Pesticide	0.0364	Production of 1 t RHs needs 1.28 kg pesticide, equaling to 6.07 kg CO_2 emissions. [14]
Diesel oil	0.737	Production of 1 t RHs needs diesel oil 33.79 kg, equaling to 122.8 kg CO_2 emissions. [14]
RHs production	0.0154	Production of 1 t RHs consumes 10.64 kWh electricity, equaling to 2.571 kg CO_2 emissions. [15] Generation of 1 kWh electricity by a thermal power, generator leads to 0.2416 kg CO_2 emissions. [16]
Heating salt to 800°C	0.044	Calculation is based on a 1 m^3 electrolysis cell containing 0.6 t NaCl-$CaCl_2$ molten salt.

Electrode fabrication	0.61	Production of 1 kg graphite leads to 3.43 kg CO_2 emissions. [17]
Anodic CO_2 produced during electrolysis in molten salts	0.557	Production of 1 kg photocatalysts leads to 0.557 kg CO_2 emissions.
Electricity required for electrolysis	1.02	Production of 1 kg photocatalysts consumes 4.22 kWh electricity and leads to 1.02 kg CO_2 emissions.
Overall	0.02	

Note: molten salt is not consumed during electrolysis, therefore the CO_2 equivalent emissions and energy equivalent input caused by molten salt are not considered. The heat need for increasing the temperature of reactant is calculated as following equation:

$$H(T) = H_f(298.15) + \int_{298.15}^{T} C_p dT + \sum H_{tr}$$

where H_f(298.15) is the enthalpy of formation at 298.15 K, Cp is the specific capacity and H_{tr} is the enthalpy of transformation of the substance. The upstream data is acquired from the HSC software.

Table S9. Calculations details of LCA for the SiC/C photocatalyst production.

Content	CO_2 equivalent emission ($t_{CO2}\ t_{SiC/C}^{-1}$)	Note
CO_2 fixed by rice husk production	−4.51	The carbon content in RHs is 20.5 wt.%, production of 1 kg RHs needs 0.7517 kg CO_2. [1]
Fertilizer	1.51	Production of 1 t RHs needs 4 t rice theoretically, production of 1 t photocatalysts needs 6 t RHs. [13] Production of 1 t RHs needs 59.07 kg fertilizer, equaling to 251.42 kg CO_2 emissions. [14]
Pesticide	0.0364	Production of 1 t RHs needs 1.28 kg pesticide, equaling to 6.07 kg CO_2 emissions. [14]
Diesel oil	0.737	Production of 1 t RHs needs diesel oil 33.79 kg, equaling to 122.8 kg CO_2 emissions. [14]
RHs production	0.0154	Production of 1 t RHs consumes 10.64 kWh electricity, equaling to 2.571 kg CO_2 emissions. [15] Generation of 1 kWh electricity by a thermal power, generator leads to 0.2416 kg CO_2 emissions. [16]
Heating salt to 800°C	0.044	Calculation is based on a 1 m^3 electrolysis cell containing 0.6 t NaCl-$CaCl_2$ molten salt.

Electrode fabrication	0.61	Production of 1 kg graphite leads to 3.43 kg CO_2 emissions. [17]
Anodic CO_2 produced during electrolysis in molten salts	0.57	Production of 1 kg photocatalysts leads to 0.557 kg CO_2 emissions.
Electricity required for electrolysis	1.15	Production of 1 kg photocatalysts consumes 4.22 kWh electricity and leads to 1.02 kg CO_2 emissions.
Overall	0.163	

References

[1] W. Weng, S. Wang, W. Xiao, X. W. Lou, Adv. Mater., 2020, **32**, 2001560.

[2] L. Lu, S. Wang, C. Zhou, Z. Shi, H. Zhu, Z. Xin, X. Wang, S. Yan, Z. Zou, J. Mater. Chem. A, 2018, **6**, 14838-14846.

[3] J. Yu, J. Low, W. Xiao, P. Zhou, M. Jaroniec, J. Am. Chem. Soc., 2014, **136**, 8839-8842.

[4] L. Pei, Y. Yuan, W. Bai, T. Li, H. Zhu, Z. Ma, J. Zhong, S. Yan, Z. Zou, ACS Catal., 2020, **10**, 15083-15091.

[5] L. Lu, B. Wang, S. Wang, Z. Shi, S. Yan, Z. Zou, Adv. Funct. Mater., 2017, **27**, 1702447.

[6] P. Li, Y. Zhou, Z. Zhao, Q. Xu, X. Wang, M. Xiao, Z. Zou, J. Am. Chem. Soc., 2015, **137**, 9547-9550.

[7] Y. Zhao, G. Chen, T. Bian, C. Zhou, G. I. Waterhouse, L. Z. Wu, C. H. Tung, L. J. Smith, D. O'Hare, T. Zhang, Adv. Mater., 2015, **27**, 7824-7831.

[8] R. Li, J. Hu, M. Deng, H. Wang, X. Wang, Y. Hu, H. L. Jiang, J. Jiang, Q. Zhang, Y. Xie, Y. Xiong, Adv. Mater., 2014, **26**, 4783-4788.

[9] K. Teramura, S. Iguchi, Y. Mizuno, T. Shishido, T. Tanaka, Angew. Chem. Int. Ed., 2012, **51**, 8008-8011.

[10] M. Gao, J. Yang, T. Sun, Z. Zhang, D. Zhang, H. Huang, H. Lin, Y. Fang, X. Wang, Appl. Catal. B: Environ., 2019, **243**, 734-740.

[11] Z. Xu, Y. Lin, M. Yin, H. Zhang, C. Cheng, L. Lu, X. Xue, H. J. Fan, X. Chen, D. Li, Adv. Mater. Interfaces, 2015, **2**, 1500169.

[12] L. Patrick, W. J. Choyke, Phys. Rev. B, 1970, **2**, 2255-2256.

[13] N. Soltani, A. Bahrami, M. I. Pech-Canul, L. A. González, Chem. Eng. J., 2015, **264**, 899-935.

[14] G. A. Blengini, M. Busto, J. Environ. Manag., 2009, **90**, 1512-1522.

[15] P. Roy, N. Shimizu, H. Okadome, T. Shiina, T. Kimura, J. Food Eng., 2017, **79**, 1250-1255.

[16] E. Cetinkaya, I. Dincer, G. F. Naterer, Int. J. Hydrogen Energy, 2012, **37**, 2071-2080.

[17] L. Pourzahedi, M. J. Eckelman, Environ. Sci.: Nano, 2015, **2**, 361-369.